HTML ABSTRACT + LINKS

ZnO nanowire field-effect transistor and oxygen sensing property

Zhiyong Fan, Dawei Wang, Pai-Chun Chang, Wei-Yu Tseng, and Jia G. Lu[a)]
Department of Chemical Engineering and Materials Science, and Department of Electrical Engineering and Computer Science, University of California, Irvine, California 92697

(Received 25 March 2004; accepted 20 October 2004)

Single-crystal ZnO nanowires are synthesized using a vapor trapping chemical vapor deposition method and configured as field-effect transistors. Electrical transport studies show *n*-type semiconducting behavior with a carrier concentration of $\sim 10^7\ \mathrm{cm}^{-1}$ and an electron mobility of $\sim 17\ \mathrm{cm}^2/\mathrm{V\,s}$. The contact Schottky barrier between the Au/Ni electrode and nanowire is determined from the temperature dependence of the conductance. Thermionic emission is found to dominate the transport mechanism. The effect of oxygen adsorption on electron transport through the nanowires is investigated. The sensitivity to oxygen is demonstrated to be higher with smaller radii nanowires. Moreover, the oxygen detection sensitivity can be modulated by the gate voltage. These results indicate that ZnO holds high potential for nanoscale sensing applications. © *2004 American Institute of Physics*. [DOI: 10.1063/1.1836870]

Quasi-one-dimensional ZnO nanostructures, such as nanowires, nanobelts, and nanoneedles, are attracting tremendous research interests.[1–3] As a II-VI compound semiconductor with a wide band gap (3.37 eV), ZnO nanowires (NWs) are emerging as candidates for nanoscale ultraviolet (UV) lasers, light-emitting diodes, photodetectors and chemical senors.[4–7] Although investigations of electrical transport through individual ZnO NWs were recently reported,[8,9] carrier concentrations and mobilities in such NWs have not been explored in detail. In our work, ZnO NWs were synthesized via a vapor trapping chemical vapor deposition (CVD) method.[10] Individual NWs were then configured as field-effect transistors (FETs), and the electron concentration and mobility were determined. Furthermore, the effects of oxygen adsorption on the NW electrical behavior were investigated and the oxygen sensing characteristics were quantified. The results show that ZnO NWs can serve as potential building blocks for nanoscale electronic and sensing devices.

ZnO NWs have been synthesized by other groups using various methods, such as CVD, physical deposition, and electrodeposition.[11–13] In our work, we have modified the CVD synthesis approach with a vapor trapping method. Field emission scanning electron microscopy (FE-SEM) images [Fig. 1(a)] show that the ZnO NWs are uniformly distributed in the area seeded with gold nanoparticles. NWs were formed with an average diameter of 60 nm, and lengths up to several tens of microns. Most of the NWs were observed to terminate with gold nanoparticles [see inset of Fig. 1(a)] suggesting that the synthesis mechanism is mainly the well-documented nanoparticle catalytic vapor–liquid–solid mechanism.[4,11,14] High-resolution transmission electron microscopy (HRTEM) images and electron diffraction patterns [see Fig. 1(b)] confirm that the ZnO NWs are single-crystalline. The distance between the adjacent lattice planes is 0.506 nm, in good agreement with the *c*-axis lattice constant of hexagonal ZnO ($c = 0.5195$ nm). This finding suggests that the synthesized ZnO NWs are grown along the [001] direction.

To fabricate FETs, ZnO NWs were first removed from the substrate by sonicating the Si chip in isopropyl alcohol. The resulting NW suspension was then deposited onto another silicon substrate—a degenerately doped *p*-type substrate capped with a 500 nm oxide layer. Photolithographic masking techniques were utilized to define a square array of $100\ \mu\mathrm{m}^2$ areas with 3–5 μm distance between neighboring squares. This array forms the electrodes using a bilayer evaporation of 10 nm of Ni followed by 100 nm of Au. Individual NWs with good contacts on both ends were located using a high magnification optical microscope. ZnO NW FETs were thus obtained, with metal contacts functioning as source and drain electrodes and with the Si substrate as a back gate. The inset of Fig. 2(a) shows a scanning electron microscopy (SEM) image of such a ZnO NW FET. Note that the channel length between the electrodes is 7.0 μm. Figure 2(a) displays seven current vs drain–source bias (I–V_{ds}) curves obtained under different gate voltages (V_g) varying from −6 V to 6 V. The conductance obtained from the linear region of I–V_{ds} curves, in the drain–source bias range of ±100 mV, increased from 5.7×10^{-9} S at $V_g = -6$ V to 2.12×10^{-7} S at $V_g = +6$ V. This behavior shows that the ZnO NW FET is an *n*-channel device. The I–V_{ds} curves are not symmetric and saturation regions exist at positive values of drain–source bias. When the source is

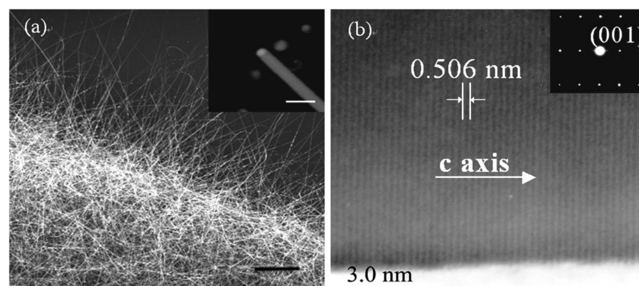

FIG. 1. (a) FE-SEM image of as-grown ZnO NWs, scale bar is 20 μm. Inset image shows a single ZnO NW terminated with a gold nanoparticle, scale bar is 100 nm. (b) HRTEM image and diffraction pattern of a ZnO NW.

[a)]Author to whom correspondence should be addressed; electronic mail: jglu@uci.edu

0003-6951/2004/85(24)/5923/3/$22.00 © 2004 American Institute of Physics
Downloaded 15 Jun 2010 to 143.89.46.199. Redistribution subject to AIP license or copyright; see http://apl.aip.org/apl/copyright.jsp

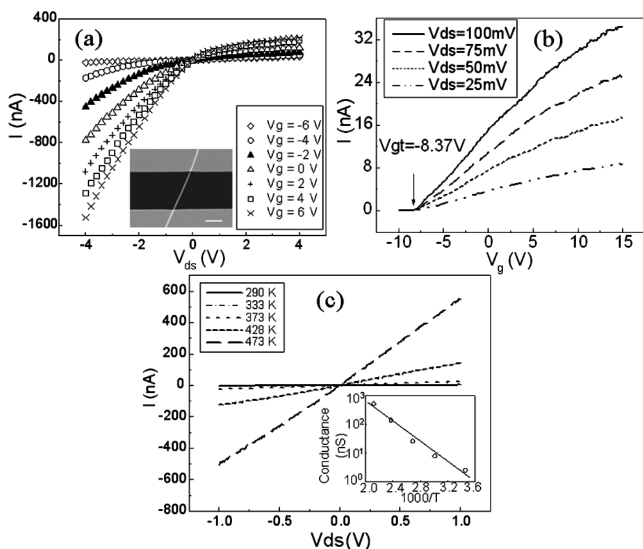

FIG. 2. (a) Room-temperature I–V_{ds} curves obtained at different gate voltages. Inset: SEM image of a ZnO NW FET with source and drain electrodes, scale bar is 2 μm. (b) Transconductance of the ZnO NW FET under 100, 75, 50, and 25 mV bias voltage. (c) I–V_{ds} curves obtained at different temperatures at $V_g = 0$ V. Inset: Conductance of NW device vs inverse temperature.

grounded and the drain is positively biased, electrons will be locally depleted near the drain, giving rise to a pinch-off effect restricting the drain–source current and the observed saturation. As shown in Fig. 2(b), transfer characteristics of this NW FET were obtained under different biases varying from 100 mV to 25 mV, and an on/off ratio for this device at 100 mV bias exceeds 10^4 (comparing $V_g = 15$ V and -10 V). According to Ref. 15, the charge carrier concentration, n, for a quasi-one-dimensional system is expressed as $n = (V_{gt}/e) \times (2\pi\varepsilon\varepsilon_0/\ln(2h/r))$, where V_{gt} is the gate threshold voltage obtained from transconductance, $\varepsilon = 3.9$, h is the gate oxide layer thickness, and r is the nanowire radius. Using $h = 500$ nm, $r = 60$ nm, and a V_{gt} value obtained from Fig. 2(b), the charge carrier concentration was estimated to be 4.0×10^7 cm^{-1}. In addition, an electron mobility of $\mu_e = 17.2$ cm^2/V s can be derived using $\mu_e = (dI/dV_g)/(2\pi\varepsilon\varepsilon_0 V_{ds}/L \ln(2h/r))$, where the transconductance $dI/dV_g = 1.9 \times 10^{-9}$ A/V was obtained from the linear region ($-5V$ to $0V$) of Fig. 2(b) (at $V_{ds} = 100$ mV) and $L = 7.0$ μm is the NW channel length. It is known that native defects of zinc interstitials contribute to the n-type semiconducting behavior of ZnO, and these defects serve as shallow donors with a binding energy of 30–60 meV.[16] The vapor trapping synthesis introduces a large number of zinc interstitials into the ZnO NWs and enhances the n-type behavior. To characterize the contact barrier between the electrodes and ZnO NW, I–V_{ds} curves were obtained under a vacuum at different temperatures, as shown in Fig. 2(c). Electrical current was observed to increase monotonically with temperature. The semilogarithmic plot of the conductance versus reciprocal temperature (I/T) [inset of Fig. 2(c)] agrees well with the thermionic emission model, in which the current $I \propto \exp(-\phi_b/k_B T)[\exp(qV_{ds}/k_B T) - 1]$. The effective energy barrier height was extracted from the slope as $\phi_b = 0.30$ eV.

It has been observed that the ambient oxygen partial pressure has a considerable effect on the performance of ZnO NW FETs. This is mainly due to conductivity changes caused by surface bandbending, induced by O_2 molecule adsorption. It is known that surface defects of metal oxides, such as oxygen vacancies, function as adsorption sites.[17,18] O_2 molecules absorbed at these sites act as electron acceptors to form O_2^- at room temperature.[19] These chemisorbed O_2^- deplete the surface electron states and consequently reduce the channel conductivity, as illustrated in the inset of Fig. 3(b). Compared with bulk materials, such a surface effect is more significant on nanowire conductance, since the surface-to-volume ratio of the nanowire is much larger. The electron depletion also affects the gate threshold voltage V_{gt} which is proportional to the carrier concentration.[15] Figure 3(a) shows a ZnO NW FET as a depletion mode device, with gate threshold voltage $V_{gt} = -1.43$ V at 10^{-2} Torr. When this device was exposed to 380 Torr or one atmosphere air (20% O_2), it became an enhanced mode device and its threshold voltage shifted from $+1.95$ V to $+3.05$ V, respectively. The inset I–V curves ($V_g = 0$ V) in Fig. 3(a) show that the corresponding current decreases when air pressure increases. The change of carrier concentration for this NW sample, with a diameter of 66 nm, was estimated to be 1.7×10^7 cm^{-1} as the pressure changed from atmosphere to 10^{-2} Torr. It was also observed that thinner ZnO NWs exhibit a higher sensitivity to the O_2 ambient. Figure 3(b) shows the NW radius dependence of the relative conductance change from atmosphere to 10^{-2} Torr. G_0 is the conductance under 10^{-2} Torr and ΔG is the conductance change from atmosphere to vacuum. As shown, $\Delta G/G_0$ increases as the NW radius decreases. This observation is mainly due to the larger surface-to-volume ratio of smaller diameter NWs.

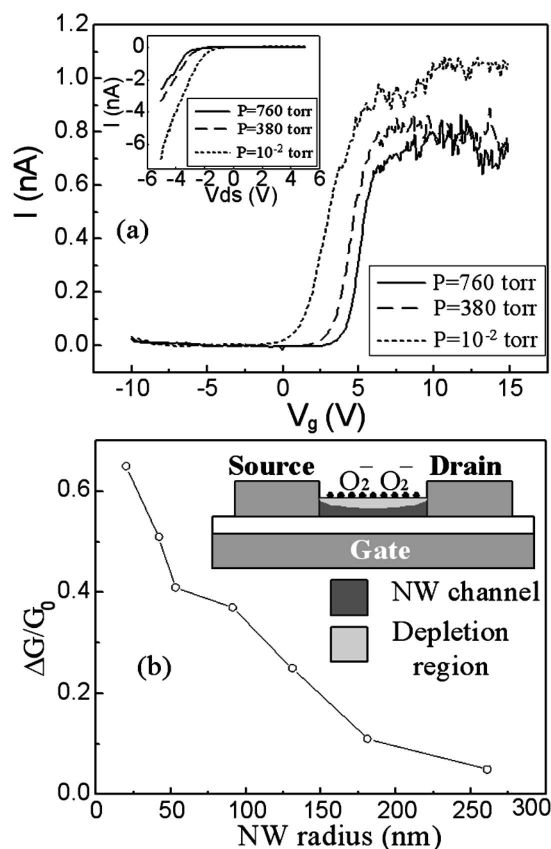

FIG. 3. (a) Transconductance of a ZnO NW FET under different pressures at room temperature, and $V_{ds} = 200$ mV. Inset: I–V_{ds} curve of the NW under 760, 380, and 10^{-2} Torr. (b) Ratio of conductance change vs radius under a vacuum and atmosphere. Inset: A schematic of NW FET channel depletion (depicted by gray shading) caused by adsorption of oxygen molecules.

Downloaded 15 Jun 2010 to 143.89.46.199. Redistribution subject to AIP license or copyright; see http://apl.aip.org/apl/copyright.jsp

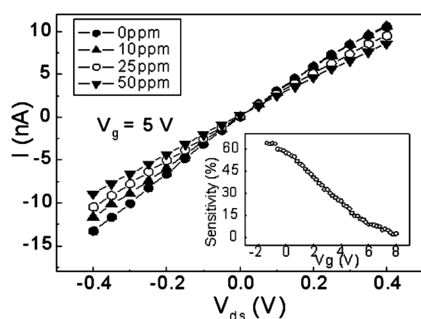

FIG. 4. I–V_{ds} curves obtained in 0, 10, 25, and 50 ppm O_2 at V_g=5 V. Conductance of ZnO NW decreases monotonically with increasing O_2 concentration. Inset: Relationship between sensitivity and gate voltage.

The principle of charge transfer between a nanostructure and its surface-adsorbed species has been utilized to realize chemical sensing with various quasi-one-dimensional systems, such as SnO_2 NWs,[18] In_2O_3 NWs,[20] and carbon nanotubes.[21] To explore the oxygen sensing properties of ZnO NWs, electrical transport was characterized under different oxygen concentrations. The NW FETs were loaded into a 1100 cm^3 chamber with electrical feedthroughs. The chamber was then pumped down to 10^{-2} Torr and baked at 120 °C for 1 h to remove any adsorbed O_2 on the NW surface. After the system was cooled to room temperature (23 °C), it was filled with 760 Torr of dilute O_2 (10–50 ppm) in a balance of Ar. The I–V_{ds} curves under different O_2 concentrations at V_g=5 V are shown in Fig. 4, which illustrates that the NW conductance decreases monotonically with increasing O_2 concentration. Sensitivity is defined as $(G_{O_2} - G_{Ar})/G_{Ar} \times 100\%$ where G_{O_2} is the conductance in diluted O_2, and G_{Ar} is the conductance in pure Ar (0 ppm O_2). It was observed that sensitivity increases as the gate voltage decreases toward the gate threshold voltage. The inset of Fig. 4 shows the relationship between sensitivity and gate voltage for 10 ppm O_2. The maximum sensitivity of 64% appears at −1.4 V, which is just above the gate threshold voltage (−2.0 V) in 10 ppm O_2. The gate dependence of O_2 detection sensitivity can be attributed to the gate modulation of the electron concentration in the NW channel. When the gate voltage is far above the threshold, electron concentration in the NW channel is quite high and the NW surface adsorbed O_2 molecules capture only a small portion of the available electrons. Therefore, the relative conductance change is very small. However, when the NW FET is gated just above the threshold, channel electrons are substantially depleted and the conductance change caused by O_2 adsorption becomes much more significant. The above results are reproducible, and show that using NW FETs as O_2 sensors take advantage of not only the large surface-to-volume ratio of the nanowires, but also the increased detection sensitivity at appropriate gate voltages. These measurement demonstrate that ZnO NWs have far better O_2 sensing performance than their thin-film counterparts,[22] as well as metal–oxide bulk material O_2 sensors,[23] at room temperature.

In summary, n-type single crystal ZnO NWs were synthesized by a vapor trapping CVD method. Electrical transport properties were investigated in fabricated NW FETs. The charge carrier concentration and electron mobility were estimated to be $\sim 10^7$ cm^{-1} and ~ 17 cm^2/V s, respectively. A contact barrier to the NWs in fabricated FET devices was characterized, and thermionic emission was found to dominate the current transport. O_2 adsorption on the NW surface was shown to have considerable effect on measured conductance, and an O_2 sensing study showed that the sensitivity depends on NW diameter as well as applied gate voltage. These results pave the way for utilizing ZnO NWs as building blocks for nanoscale electronics and chemical sensing devices.

The authors thank professor Henry P. Lee for valuable discussion and Professor Daniel Mumm for help in proofreading. Device fabrication was performed at the UC Irvine Integrated Nanosystems Research Facility. This work was supported by a NSF Grant No. ECS-0306735.

[1]H. T. Ng, B. Chen, J. Li, J. Han, M. Meyyappan, J. Wu, S. X. Li, and E. E. Haller, Appl. Phys. Lett. **82**, 2023 (2003).
[2]X. D. Bai, P. X. Gao, Z. L. Wang, and E. G. Wang, Appl. Phys. Lett. **82**, 4806 (2003).
[3]Y.-K. Tseng, C.-J. Huang, H.-M. Cheng, I.-N. Lin, K.-S. Liu, Adv. Funct. Mater. **13**, 811 (2003).
[4]P. Yang, H. Yan, S. Mao, R. Russo, J. Johnson, R. Saykally, N. Morris, J. Pham, R. He, and H.-J. Choi, Adv. Funct. Mater. **12**, 323 (2002).
[5]C. H. Liu, J. A. Zapien, Y. Yao, X. M. Meng, C. S. Lee, S. S. Fan, Y. Lifshitz, and S. T. Lee, Adv. Mater. (Weinheim, Ger.) **15**, 838 (2003).
[6]H. Kind, H. Yan, B. Messer, M. Law, and P. Yang, Adv. Mater. (Weinheim, Ger.) **14**, 158 (2002).
[7]Q. Wan, Q. H. Li, Y. J. Chen, T. H. Wang, X. L. He, J. P. Li, and C. L. Lin, Appl. Phys. Lett. **84**, 3654 (2004).
[8]Q. H. Li, Q. Wan, Y. X. Liang, and T. H. Wang, Appl. Phys. Lett. **84**, 4556 (2004).
[9]Y. W. Heo, L. C. Tien, D. P. Norton, B. S. Kang, F. Ren, B. P. Gila, and S. J. Pearton, Appl. Phys. Lett. **85**, 2002 (2004).
[10]P. Chang, Z. Fan, W. Tseng, D. Wang, W. Chiou, J. Hong, and J. G. Lu, Chem. Mater. **16**, 5133 (2004).
[11]Y. W. Wang, L. D. Zhang, G. Z. Wang, X. S. Peng, Z. Q. Chu, and C. H. Liang, J. Cryst. Growth **234**, 171 (2002).
[12]Y. C. Kong, D. P. Yu, B. Zhang, W. Fang, and S. Q. Feng, Appl. Phys. Lett. **78**, 407 (2001).
[13]M. J. Zheng, L. D. Zhang, G. H. Li, and W. Z. Shen, Chem. Phys. Lett. **363**, 123 (2002).
[14]P. X. Gao, Y. Ding, and Z. L. Wang, Nano Lett. **3**, 1315 (2003).
[15]R. Martel, T. Schmidt, H. R. Shea, T. Hertel, and P. Avouris, Appl. Phys. Lett. **73**, 2447 (1998).
[16]D. C. Look, J. W. Hemsky, and J. R. Sizelove, Phys. Rev. Lett. **82**, 2552 (1999).
[17]V. E. Henrich, P. A. Cox, *Surface Science of Metal Oxides* (Cambridge University Press, Cambridge, UK, 1994).
[18]Y. Zhang, A. Kolmakov, S. Chretien, H. Metiu, and M. Moskovits, Nano Lett. **4**, 403 (2004).
[19]F. Chaabouni, M. Abaab, and B. Rezig, Sens. Actuators B **100**, 200 (2004).
[20]D. Zhang, C. Li, X. Liu, S. Han, T. Tang, and C. Zhou, Appl. Phys. Lett. **83**, 1845 (2003).
[21]J. Kong, N. R. Franklin, C. Zhou, M. G. Chapline, S. Peng, K. Cho, and H. Dai, Science **287**, 622 (2000).
[22]A. Trinchi, Y. X. Li, W. Wlodarski, S. Kaciulis, L. Pandolfi, S. P. Russo, J. Duplessis, and S. Viticoli, Sens. Actuators, A **108**, 263 (2003).
[23]P. T. Mosley, Sens. Actuators B **6**, 149 (1992).

Downloaded 15 Jun 2010 to 143.89.46.199. Redistribution subject to AIP license or copyright; see http://apl.aip.org/apl/copyright.jsp